Understanding the shape of the galaxy two-point correlation function at z ≃ 1 in the COSMOS field

Publisher:
WILEY-BLACKWELL

Available
This version is available at 11696/71457 since: 2021-10-22T14:40:13Z

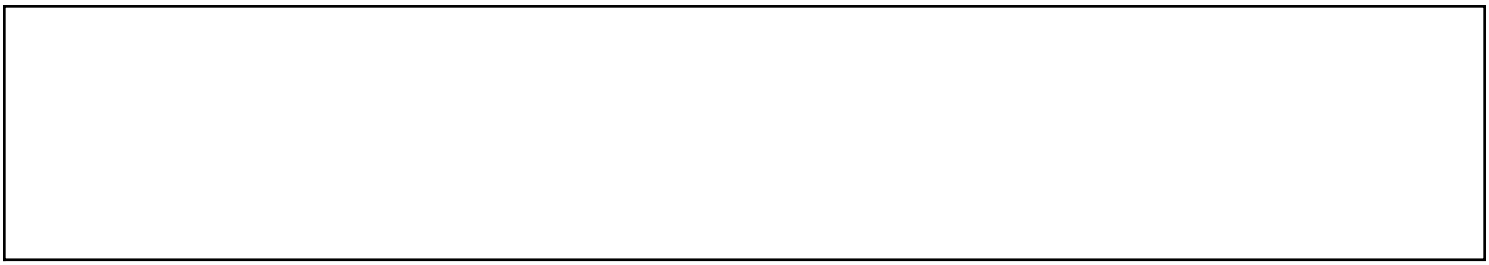

Monthly Notices
of the
ROYAL ASTRONOMICAL SOCIETY

Mon. Not. R. Astron. Soc. **409,** 867–872 (2010) doi:10.1111/j.1365-2966.2010.17352.x

Understanding the shape of the galaxy two-point correlation function at $z \simeq 1$ in the COSMOS field

S. de la Torre, [1,2]★ L. Guzzo,[1] K. Kovač, [3] C. Porciani,[4] U. Abbas,[5] B. Meneux,[6,7] C. M. Carollo,[3] T. Contini,[8] J. P. Kneib,[9] O. Le Fèvre,[9] S. J. Lilly,[3] V. Mainieri,[10] A. Renzini,[11] D. Sanders,[12] M. Scodeggio,[2] N. Scoville,[13] G. Zamorani,[14] S. Bardelli,[14] M. Bolzonella,[14] A. Bongiorno,[6] K. Caputi,[3] G. Coppa,[14] O. Cucciati,[9] L. de Ravel, [9] P. Franzetti,[2] B. Garilli,[2] A. Iovino,[1] P. Kampczyk,[3] C. Knobel,[3] A. M. Koekemoer,[15] F. Lamareille,[8] J.-F. Le Borgne,[8] V. Le Brun,[9] C. Maier,[3] M. Mignoli,[14] R. Pelló,[8] Y. Peng,[3] E. Perez-Montero,[8] E. Ricciardelli,[16] J. Silverman,[3] M. Tanaka,[10] L. Tasca,[2] L. Tresse,[9] D. Vergani,[14] N. Welikala,[9] E. Zucca,[14] D. Bottini,[2] A. Cappi,[14] P. Cassata,[17] A. Cimatti,[18] M. Fumana,[2] O. Ilbert,[9] A. Leauthaud,[19] D. Maccagni,[2] C. Marinoni,[20] H. J. McCracken,[21] P. Memeo,[2] P. Nair,[14] P. Oesch,[3] L. Pozzetti,[14] V. Presotto[1] and R. Scaramella[22]

[1]*INAF – Osservatorio Astronomico di Brera, 23807 Merate, Italy*
[2]*INAF – Istituto di Astrofisica Spaziale e Fisica Cosmica di Milano, 20133 Milano, Italy*
[3]*Institute of Astronomy, ETH Zurich, 8093 Zurich, Switzerland*
[4]*Argelander Institute for Astronomy, University of Bonn, 53121 Bonn, Germany*
[5]*INAF – Osservatorio Astronomico di Torino, 10025 Pino Torinese, Italy*
[6]*Max Planck Institut für Extraterrestrische Physik, 85748 Garching, Germany*
[7]*Universitats-Sternwarte Muenchen, 81679 Munich, Germany*
[8]*Laboratoire d'Astrophysique de l'Observatoire Midi-Pyrénées, 31400 Toulouse, France*
[9]*Laboratoire d'Astrophysique de Marseille, 13388 Marseille, France*
[10]*European Southern Observatory, 85748 Garching, Germany*
[11]*INAF – Osservatorio Astronomico di Padova, 35122 Padova, Italy*
[12]*Institute for Astronomy, University of Hawaii, 96822-1839 Honolulu, USA*
[13]*Astronomy Department, Caltech, 91125 Pasadena, USA*
[14]*INAF – Osservatorio Astronomico di Bologna, 40127 Bologna, Italy*
[15]*Space Telescope Science Institute, 21218 Baltimore, USA*
[16]*Dipartimento di Astronomia, Universitá di Padova, 35122 Padova, Italy*
[17]*Department of Astronomy, University of Massachusetts, 01003 Amherst, USA*
[18]*Dipartimento di Astronomia, Universitá di Bologna, 40127 Bologna, Italy*
[19]*Berkeley Lab & Berkeley Center for Cosmological Physics, University of California, 94720 Berkeley, USA*
[20]*Centre de Physique Théorique de Marseille, 13288 Marseille, France*
[21]*Institut d'Astrophysique de Paris, 75014 Paris, France*
[22]*INAF – Osservatorio Astronomico di Roma, 00040 Monte Porzio Catone, Italy*

Accepted 2010 July 12. Received 2010 July 7; in original form 2010 May 21

ABSTRACT

We investigate how the shape of the galaxy two-point correlation function as measured in the zCOSMOS survey depends on local environment, quantified in terms of the density contrast on scales of $5\,h^{-1}$ Mpc. We show that the flat shape previously observed at redshifts between $z = 0.6$ and 1 can be explained by this volume being simply 10 per cent overabundant in high-density environments, with respect to a universal density probability distribution function.

★E-mail: sylvain.delatorre@brera.inaf.it

When galaxies corresponding to the top 10 per cent tail of the distribution are excluded, the measured $w_p(r_p)$ steepens and becomes indistinguishable from Lambda cold dark matter (ΛCDM) predictions on all scales. This is the same effect recognized by Abbas & Sheth in the Sloan Digital Sky Survey (SDSS) data at $z \simeq 0$ and explained as a natural consequence of halo–environment correlations in a hierarchical scenario. Galaxies living in high-density regions trace dark matter haloes with typically higher masses, which are more correlated. If the density probability distribution function of the sample is particularly rich in high-density regions because of the variance introduced by its finite size, this produces a distorted two-point correlation function. We argue that this is the dominant effect responsible for the observed 'peculiar' clustering in the COSMOS field.

Key words: galaxies: evolution – galaxies: high-redshift – galaxies: statistics – cosmology: observations – large-scale structure of Universe.

1 INTRODUCTION

Advances in the spectroscopic survey capabilities of 8-m class telescopes have allowed us in the recent years to extend detailed studies of the clustering of galaxies to the $z \simeq 1$ Universe (Coil et al. 2004; Le Fèvre et al. 2005; Coil et al. 2006; Meneux et al. 2006; Pollo et al. 2006; de la Torre et al. 2007; Coil et al. 2008; Meneux et al. 2008; Abbas et al. 2010). The most recent contribution to this endeavour is the COSMOS survey (Scoville et al. 2007), and in particular zCOSMOS, its redshift follow-up with the Visible Multi-Object Spectrograph (VIMOS) at the European Southern Observatory (ESO) Very Large Telescope (VLT; Lilly et al. 2007).

Early angular studies of the COSMOS field (McCracken et al. 2007) and more recent analyses of the first 10 000 zCOSMOS redshifts to $I_{AB} = 22.5$ have evidenced significant 'excess' clustering in the large-scale shape of the two-point angular and projected correlation function. The redshift information from zCOSMOS, in particular, shows this excess to dominate in the redshift range $0.5 < z < 1$ (Meneux et al. 2009). More precisely, the shape of the projected two-point correlation function $w_p(r_p)$ appears to decay much less rapidly than observed at similar redshifts in independent data as the VIMOS VLT Deep Survey (VVDS; Meneux et al. 2008) and with respect to predictions of standard Lambda cold dark matter (ΛCDM) cosmology as incarnated by the Millennium Simulation (De Lucia & Blaizot 2007; Kitzbichler & White 2007). The observed flat shape[1] is difficult to reconcile with the theory, unless an unrealistic scale-dependent bias between galaxies and matter is advocated. While plausibly related to the presence of particularly rich large-scale structures dominating the COSMOS volume around $z \simeq 0.7$ (e.g. Guzzo et al. 2007; Meneux et al. 2009), this effect still awaits a quantitative explanation.

In a recent series of papers, Abbas & Sheth (2005, 2006, 2007) have used the Sloan Digital Sky Survey (SDSS; York et al. 2000), together with Halo Occupation Distribution (HOD) models (e.g. Cooray & Sheth 2002) to show how in general the amplitude and shape of the galaxy correlation function depend on the *environment* in which the galaxies are found. Once a local density is suitably defined over a given scale, galaxies living in overdense regions show a stronger clustering than those in average or underdense environments. This is shown to be a consequence of the direct correlation arising in hierarchical clustering between the mass of the dark matter haloes in which galaxies are embedded and their large-scale environment: the mass function of dark matter haloes is top-heavy in high-density regions, thus in selecting galaxies in these environments we are selecting haloes of higher mass, which are more clustered. The net result is to introduce a *scale-dependent bias* in the observed correlation function, when this is compared to the expected dark matter clustering (Abbas & Sheth 2006, 2007).

In this paper we investigate whether this effect is at work also at $z \simeq 0.7$ and could explain quantitatively the observed shape of $w_p(r_p)$ in the zCOSMOS data.

2 DATA AND METHODS

2.1 The zCOSMOS 10k-bright sample

zCOSMOS is a large spectroscopic survey performed with VIMOS (Le Fèvre et al. 2003) at the ESO–VLT. The zCOSMOS-bright survey (Lilly et al. 2007) has been designed to follow up spectroscopically the entire 1.7 deg^2 Hubble Space Telescope COSMOS field (Koekemoer et al. 2007; Scoville et al. 2007) down to $I_{AB} = 22.5$. We use in this analysis the first-epoch set of redshifts, usually referred to as the zCOSMOS *10k-bright sample* ('10k sample', hereafter), including 10 644 galaxies. At this magnitude limit, the survey redshift distribution peaks at $z \simeq 0.6$, with a tail out to $z \simeq 1.2$. We only consider secure redshifts, i.e. confidence classes 4.*x*, 3.*x*, 9.3, 9.5, 2.4, 2.5 and 1.5, representing 88 per cent of the full 10k sample (see Lilly et al. 2009 for details) and 20.4 per cent of the complete $I_{AB} < 22.5$ magnitude-limited parent sample over the same area. These data are publicly available through the ESO Science Data Archive site.[2]

2.2 Mock galaxy surveys

In addition to the observed data, in this analysis we also make use of a set of 24 mock realizations of the zCOSMOS survey, constructed combining the Millennium Run *N*-body simulation,[3] with a semi-analytical recipe of galaxy formation (Kitzbichler & White 2007). The Millennium Run is a large dark matter *N*-body simulation that follows the hierarchical evolution of 2160^3 particles between $z = 127$ and 0 in a cubic volume of $500^3\,h^{-3}\,\mathrm{Mpc}^3$. It assumes a

[1] $\gamma \sim 1.5$ instead of the $\gamma \sim 1.8$ expected when approximating $\xi(r)$ with a power law [i.e. $\xi(r) = (r_0/r)^\gamma$] below $r = 10\,h^{-1}$ Mpc.

[2] http://archive.eso.org/cms/eso-data/data-packages/

[3] http://www.mpa-garching.mpg.de/millennium/

concordance cosmological ΛCDM model with ($\Omega_{\rm m}$, Ω_Λ, $\Omega_{\rm b}$, h, n, σ_8) = (0.25, 0.75, 0.045, 0.73, 1, 0.9). The resolution of the N-body simulation, $8.6 \times 10^8\ h^{-1}{\rm M}_\odot$, coupled with the semi-analytical model allows one to resolve with a minimum of 100-particle haloes containing galaxies with a luminosity of $0.1L^*$ (see Springel et al. 2005). Galaxies are generated inside these dark matter haloes using the semi-analytic model of Croton et al. (2006), as improved by De Lucia & Blaizot (2007). This model includes the physical processes and requirements originally introduced by White & Frenk (1991) and refined by Kauffmann & Haehnelt (2000), Springel et al. (2001), De Lucia et al. (2004) and Springel et al. (2005). The 24 mocks are created then 'observed' as to reproduce the zCOSMOS selection function (Iovino et al. 2010).

2.3 Local density estimator

To characterize galaxy environment we use the dimensionless density contrast measured by Kovač et al. (2010) around each galaxy in the sample. For each galaxy at a comoving position $\boldsymbol{r}$ we compute the dimensionless 3D density contrast smoothed on a scale R, $\delta_{\rm g}(\boldsymbol{r}, R) = [\rho(\boldsymbol{r}, R) - \bar{\rho}(\boldsymbol{r})]/\bar{\rho}(\boldsymbol{r})$, where $\rho(\boldsymbol{r}, R)$ is the density of galaxies measured on a scale R and $\bar{\rho}(\boldsymbol{r})$ is the overall mean density at $\boldsymbol{r}$. $\rho(\boldsymbol{r}, R)$ is estimated around each galaxy of the sample by counting objects within an aperture (defined either through a top hat of size R or a Gaussian filter with similar dispersion). The reconstructed overdensities are properly corrected for the survey-selection function and edge effects. Kovač et al. (2010) studied different density estimators, corresponding to varying galaxy tracers, filter shapes and smoothing scales. Here we use $\delta_{\rm g}$ as reconstructed with a Gaussian filter with dispersion $R = 5\,h^{-1}$ Mpc. Note that the mass enclosed by such filter is equal to that inside a top-hat filter of size $\sim 7.8\,h^{-1}$ Mpc. We refer the reader to Kovač et al. (2010) for a full description of the technique.

2.4 Expected probability distribution function of the density contrast

The density contrast distribution can be predicted analytically using some approximations. Empirically, it has been found that the probability distribution function (PDF) of the mass density contrast in real (comoving) space smoothed on a scale R is well described by a lognormal distribution (Coles & Jones 1991),

$$P(\delta) = \frac{(2\pi\omega_R^2)^{-1/2}}{1+\delta} \exp\left\{-\frac{[\ln(1+\delta)+\omega_R^2]^2}{2\omega_R^2}\right\}, \quad (1)$$

where $\omega_R^2 = \ln(1 + \langle\delta^2\rangle_R)$ and $\langle\delta^2\rangle_R = \sigma_R^2(z)$, with $\sigma_R(z)$ being the standard deviation of mass fluctuations at redshift z on the same scale:

$$\sigma_R^2(z) = \int_0^\infty \frac{{\rm d}k}{k} \frac{k^3 P(k,z)}{2\pi^2} |W(kR)|^2. \quad (2)$$

Here $P(k, z)$ is the mass power spectrum at redshift z in the adopted cosmology and $W(x)$ is the Fourier transform of the smoothing window function. For our purpose we use the mass power spectrum of Smith et al. (2003), which includes the non-linear evolution of the initial mass fluctuations field.

The density field recovered from redshift surveys is affected by galaxy peculiar motions. Therefore one needs to convert the real-space PDF model into redshift space in order to be able to compare it to observations. It has been found that the redshift-space PDF of the density contrast is still well described by a lognormal distribution (Sigad, Branchini & Dekel 2000), with a standard deviation $\sigma_R^z(z)$ related to that in real space as (Kaiser 1987)

$$\sigma_R^z(z) = \left(1 + \frac{2}{3}f(z) + \frac{1}{5}f^2(z)\right)^{1/2} \sigma_R(z). \quad (3)$$

Here σ_R and σ_R^z are, respectively, the real- and redshift-space standard deviations and $f(z)$ denotes the growth rate of structure, which in the framework of general relativity is well approximated as $f(z) \simeq \Omega_{\rm m}^{0.55}(z)$ (Wang & Steinhardt 1998).

Following this procedure we obtain the PDF of the mass density contrast in redshift space. To obtain that of galaxies we have to further apply a biasing factor. For our purposes here, we simply assume linear deterministic biasing, setting $\delta_{\rm g} = b\delta$ (however, see Marinoni et al. 2005). We choose a value $b = \sqrt{2.05}$, as required to match the large-scale amplitude of the two-point correlation function of galaxies in our sample, as we shall show in Section 3.

By definition, the PDF described by equation (1) refers to the distribution of δ as measured in randomly placed spheres within the survey volume. On the other hand, for the data we have at our disposal only the *conditional* values of $\delta_{\rm g}$ as measured in volumes centred on each galaxy in the sample. Given the probabilistic meaning of the distribution function of the density $\mathcal{P}(\rho)$ in the two cases they must be related as

$$\mathcal{P}_c(\rho) = \frac{\rho\mathcal{P}(\rho)}{\int_0^\infty \rho\mathcal{P}(\rho){\rm d}\rho} = \frac{\rho}{\bar{\rho}}\mathcal{P}(\rho). \quad (4)$$

Being $P(\delta) = \bar{\rho}\mathcal{P}(\rho)$, the corresponding relation between the PDFs of the density contrast $P(\delta)$ is

$$P_c(\delta) = \frac{(1+\delta)P(\delta)}{\overline{1+\delta}}, \quad (5)$$

where $\overline{1+\delta} = 1$.

We are then in the position to compare the theoretically predicted P_c (normalized to the total number of galaxies in the sample) to the observed distribution. This is presented in Fig. 1, together with the mean and scatter (68 per cent confidence corridor) of the 24 mock samples. The analytical prediction and the mean of the mocks are in fair agreement (although they disagree in the details at the 1σ level). Note, however, that the detailed shape and amplitude of the analytical prediction are quite sensitive to the choice of the effective redshift $\bar{z}$ of the survey. Here we have used the mean value $\bar{z} \simeq 0.56$ yielded by the actual redshift distribution ${\rm d}\,N/{\rm d}\,z$ of the survey, but using e.g. $\bar{z} \simeq 0.6$ would give a better agreement with the PDF from the simulations. Additionally, the analytical prediction cannot include the small-scale 'finger-of-God' effect due to high velocities in clusters (which however has the effect to reduce power on small scales). Finally, it has been computed using the more up-to-date $\sigma_8 = 0.8$, to check the impact of the value $\sigma_8 = 0.9$ used for the Millennium Run. Beyond these points, the simple goal of the analytical model is to show an alternative – yet more idealized – example, in addition to the mocks, of what one should expect from the theory. What is relevant for this paper is that the conditional PDF of the data differs strongly from both theoretical predictions. Peaking at $\delta_{\rm g} \simeq -0.2$, it shows an extended high-density tail out to $\delta_{\rm g} \simeq 7$. The distribution expected from the models is more peaked around $\delta_{\rm g} = 0$ and drops more rapidly for $\delta_{\rm g} > 2$. This plot clearly

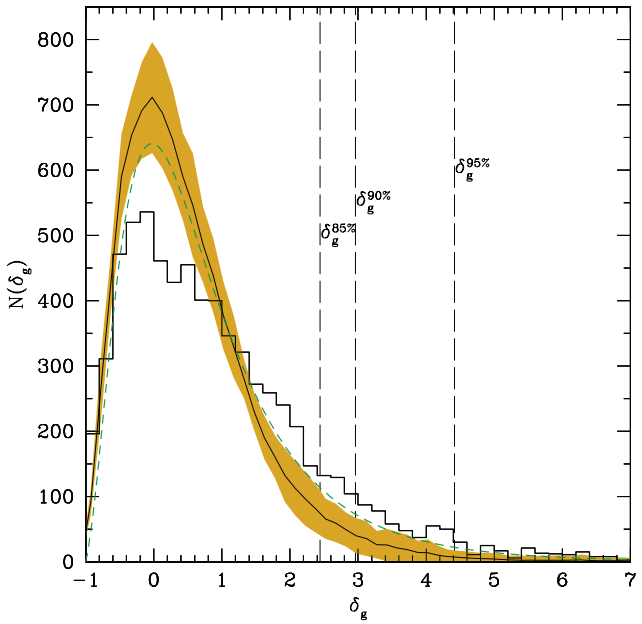

Figure 1. The PDF of the density contrast, measured around each galaxy in the current zCOSMOS 10k catalogue as discussed in the text (histogram). The solid line and shaded area correspond, respectively, to the mean and 1σ dispersion of the same statistics, measured on the 24 Millennium mocks; the dashed curve gives instead, as reference, the expected theoretical distribution for a lognormal model in a ΛCDM cosmology with $(\Omega_m,\ \Omega_\Lambda,\ \sigma_8) = (0.25, 0.75, 0.8)$, at the mean redshift of the 10k sample, computed as discussed in the text. The vertical solid lines correspond to values of the density contrast excluding the top 5, 10 and 15 per cent of the distribution.

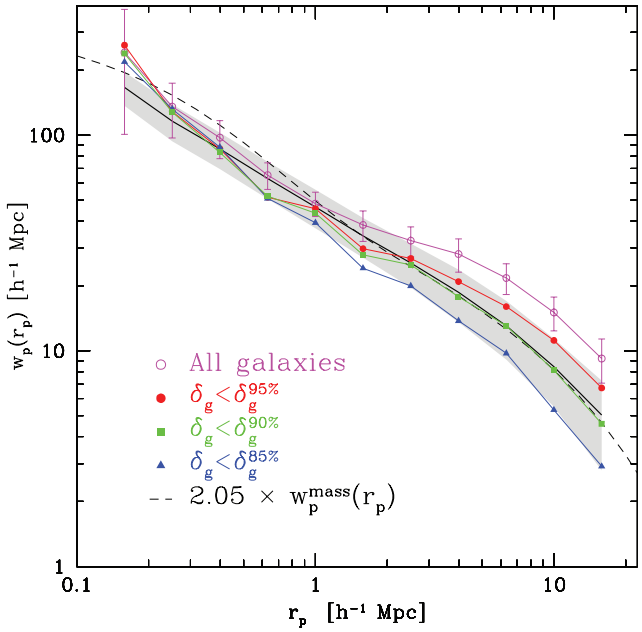

Figure 2. The projected two-point correlation function $w_p(r_p)$ of the zCOSMOS 10k at $0.6 < z < 1$, compared to subsamples in which galaxies living in the densest environments are gradually excluded (top to bottom). To reduce confusion, error bars are shown for the main sample only, being in general of amplitude comparable to the scatter of the mock samples indicated by the shaded area. The thick solid line and surrounding shaded corridor correspond in fact to the mean and 1σ scatter of the 24 mock surveys. For comparison, the dashed curve also shows the HALOFIT (Smith et al. 2003) analytic prescription for the non-linear mass power spectrum [assuming ΛCDM with $(\Omega_m,\ \Omega_\Lambda,\ \sigma_8) = (0.25, 0.75, 0.8)$], multiplied by an arbitrary linear bias $b^2 = 2.05$. The shape of $w_p(r_p)$ for zCOSMOS galaxies agrees with the models when the 10 per cent densest environments are eliminated.

shows a statistically significant excess of high-density regions in the galaxy data.[4]

2.5 Clustering estimation

We estimate real-space galaxy clustering using the standard projected two-point correlation function, $w_p(r_p)$, that properly corrects for redshift-space distortions due to galaxy peculiar motions. This is obtained by projecting the 2D two-point correlation function $\xi(r_p, \pi)$ along the line of sight[5]

$$r_p(r_p) = 2\int_0^\infty \xi(r_p, \pi)\mathrm{d}\pi, \qquad (6)$$

where r_p and π are the components of the galaxy–galaxy separation vector, respectively, perpendicular and parallel to the line of sight (Peebles 1980; Fisher et al. 1994). $\xi(r_p, \pi)$ is measured using the Landy & Szalay (1993) estimator and properly accounting for the survey selection function and various incompleteness effects, as thoroughly described in de la Torre et al. (2009). Error bars are estimated through the blockwise bootstrap method (e.g. Porciani & Giavalisco 2002; Norberg et al. 2009). This is discussed in detail and compared to results from mock samples in Meneux et al. (2009) and Porciani et al. (in preparation). All clustering codes and methods used here have been extensively tested against independent programs in the course of the latter analyses.

3 RESULTS AND DISCUSSION

In Fig. 2 we show the projected correlation function $w_p(r_p)$ computed for the 10k sample in the redshift range $0.6 < z < 1$ (top curve), together with those from a series of subsamples in which we gradually eliminated galaxies located in the most dense environments. We excluded, respectively, the top 5, 10, and 15 per cent fractions of the distribution of overdensities, corresponding to the dashed vertical lines in Fig. 1. $w_p(r_p)$ for the full 10k sample shows a very flat shape, with significant 'excess clustering' above $1\,h^{-1}$ Mpc, as seen in previous analyses of the COSMOS/zCOSMOS data. When galaxies in the densest environments are excluded, however, the large-scale 'shoulder' gradually disappears. What we see is a clear dependence of the mean large-scale clustering of galaxies on the type of environments they inhabit, similarly to the results of Abbas & Sheth (2007) from the SDSS.

[4] An ongoing analysis of the fuller COSMOS sample to $I_{AB} = 24$ based on photometric redshifts (Scoville et al., in preparation) seems to indicate a better agreement of the observed PDF to that of the Millennium mocks. This might be explained as a consequence of the larger volume of the sample used (lower cosmic variance), together with the fairly large smoothing window used to define the overdensities and, most importantly, the blurring of the PDF produced by the photometric redshift errors.

[5] In practice, a finite value for the upper integration limit is adopted. We use $20\,h^{-1}$ Mpc which recovers the signal dispersed by redshift distortions, while minimizing the noise that dominates at large values of π (see also Meneux et al. 2009; Porciani, in preparation).

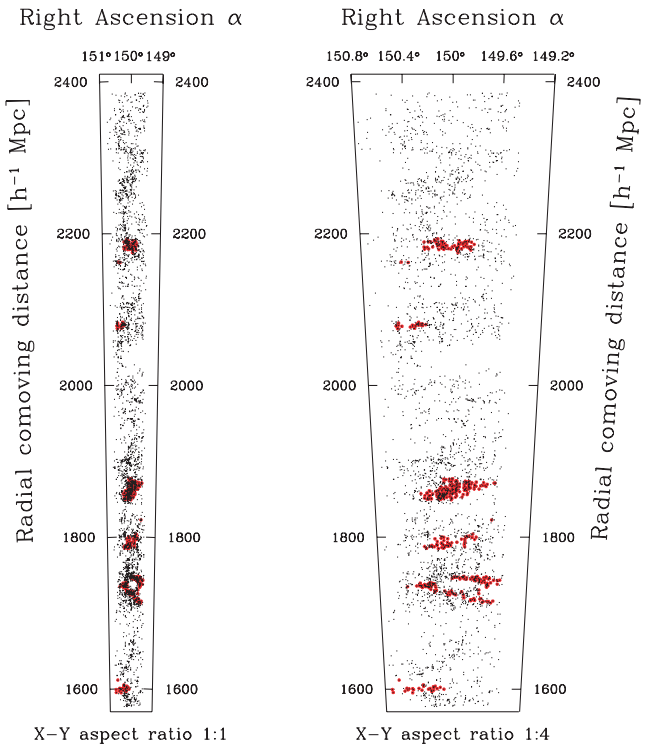

Figure 3. The spatial distribution of galaxies with $0.6 < z < 1$ (dots) in the zCOSMOS 10k sample, highlighting those inhabiting the 10 per cent highest density tail of the distribution (circles). These galaxies clearly belong to a few well-defined structures. The right-hand plot is simply an expanded version of the pencil beam on the left-hand side to enhance visibility.

In the same figure we also show the 'universal' $w_p(r_p)$ expected in the standard ΛCDM cosmological model with linear biasing. The theory predictions are, again, obtained in two ways. First, we use HALOFIT (Smith et al. 2003) to compute directly the approximated non-linear mass power spectrum expected at the survey mean redshift. Secondly, we compute the average and scatter of $w_p(r_p)$ from the 24 mock samples. Remarkably, the two curves (solid and dashed black lines) are virtually indistinguishable above $1\,h^{-1}$ Mpc once the HALOFIT mass correlation function is properly multiplied by an arbitrary linear bias factor of $b^2 = 2.05$. The comparison to the data shows a very good agreement for the 10k subsample in which the 10 per cent densest environments were excluded. We note that the shape of $w_p(r_p)$ measured from the independent VVDS survey shows a shape which is closer to the model predictions (Meneux et al. 2009). With this thresholding in density of the 10k data, therefore, we are able to bring the measured shape of galaxy clustering at $z \simeq 0.7$ from zCOSMOS, VVDS and the standard cosmological model within close agreement, suggesting a more quantitative interpretation of the flat shape of $w_p(r_p)$ observed in zCOSMOS at these redshifts. In previous papers (e.g. Kovač et al. 2009; Meneux et al. 2009) we already suggested that this could be due to the presence of particularly significant large-scale structures between $z = 0.5$ and 1. Here we see that it is in fact driven by an excess of galaxies sampling high-density regions, skewing the density distribution away from the supposedly 'universal' shape. Fig. 3 shows where these high-density galaxies are actually located within the 10k sample. The galaxies belonging to the 10 per cent high-density tail are marked by (red) circles and turn out to belong to a few very well-defined structures only.[6] It is easy to imagine that if embedded in a larger volume, these structures would not weight so much as to modify significantly the overall shape of the PDF. As seen from the histogram in Fig. 1, in this volume they produce a clear overabundance of high-density galaxy environments, while regions with average density are under-represented.

One may wonder, however, whether the theoretical model represented by the Millennium mocks can be taken as a reliable reference. In fact, it has been shown that this specific model tends to overestimate the overall amplitude of $w_p(r_p)$ at $z \simeq 1$ and does not reproduce the observed clustering segregation in colour (e.g. Coil et al. 2008; de la Torre et al., in preparation) In general, semi-analytical recipes do tend to affect the amplitude and shape of the correlation function. This however happens only on small scales, where the complex interplay between galaxy formation processes and the distribution of dark matter haloes has an impact. On large scales instead, they predict a fairly linear biasing, as we can see directly comparing the solid and dashed black lines in Fig. 2. This means that the large-scale shape of the correlation function is essentially driven by the underlying mass distribution in the assumed cosmological model and not by the details of the semi-analytic recipe adopted to generate galaxies. A different recipe would not affect, therefore, the results obtained here, unless we postulate the existence of dramatically non-local galaxy formation processes (e.g. Narayanan, Berlind & Weinberg 2000).

We also note from Fig. 2 that the dependence of $w_p(r_p)$ on the PDF threshold is essentially on large scales. Below $\sim 1\,h^{-1}$ Mpc there is no significant change when denser and denser environments are excluded. In their analysis of the SDSS, Abbas & Sheth (2007) consider subsamples defined as extrema of the density distribution, i.e. using galaxies lying on the tails of the distribution on both sides. With this selection, they do find a change in $w_p(r_p)$ for different environments also on small scales. It can be shown simply using the conservation of galaxy pairs (see equation 1 of Abbas & Sheth 2007) that the two results are in fact consistent with each other (Ravi Sheth, private communication).

These results highlight the importance in redshift surveys of an accurate reconstruction of the density field to evidence possible peculiarities in the overall PDF as sampled by that specific catalogue. Further strengthening the results obtained by Abbas & Sheth (2007) at $z \simeq 0$, we have shown that an anomalous density distribution function can significantly bias the recovered two-point correlation function, making it difficult to draw general conclusions from its shape. This result provides another example of the intrinsic difficulty existing when comparing observations of the galaxy distribution to theoretical predictions. The theory provides us with fairly accurate forecasts for the distribution of the dark matter and for that of the haloes within which we believe galaxies form (e.g. Mo, Jing & White 1996; Sheth & Tormen 1999). However, translating galaxy clustering measurements into constraints for the halo clustering involves understanding of how the selected galaxies populate haloes with different mass. The result presented here shows how a sample particularly rich in dense structures favours higher mass haloes, which in turn are more clustered, thus biasing the observed correlation function as a function of scale. A more detailed analysis of the

[6] We also directly tested whether the two-point correlation functions computed on the density-thresholded samples were by any means sensitive to the way the 'depleted' subvolumes were treated (e.g. kept in or excluded when building the standard reference random sample); no significant changes were found.

environmental dependence of galaxy clustering in the zCOSMOS-bright sample and related HOD modelling will be presented in a future paper.

ACKNOWLEDGMENTS

We thank Ravi Sheth for helpful comments on the manuscript, and M. Kitzbichler and S. White for providing us with the COSMOS mock surveys. LG thanks D. Sanders and the University of Hawaii for hospitality at the Institute for Astronomy, where this work was initiated. Financial support from INAF and ASI through grants PRIN-INAF–2007 and ASI/COFIS/WP3110 I/026/07/0 is gratefully acknowledged.

This work is based on observations undertaken at the ESO–VLT under Large Programme 175.A-0839. Also based on observations with the NASA/ESA *Hubble Space Telescope*, obtained at the Space Telescope Science Institute, operated by the Association of Universities for Research in Astronomy, Inc. (AURA), under NASA contract NAS 5Y26555, with the Subaru Telescope, operated by the National Astronomical Observatory of Japan, with the telescopes of the National Optical Astronomy Observatory, operated by the Association of Universities for Research in Astronomy, Inc. (AURA), under cooperative agreement with the National Science Foundation and the Canada–France–Hawaii Telescope, operated by the National Research Council of Canada, the Centre National de la Recherche Scientifique de France and the University of Hawaii.

REFERENCES

Abbas U., Sheth R. K., 2005, MNRAS, 364, 1327
Abbas U., Sheth R. K., 2006, MNRAS, 372, 1749
Abbas U., Sheth R. K., 2007, MNRAS, 378, 641
Abbas U. et al., 2010, MNRAS, 406, 1306
Coil A. L. et al., 2004, ApJ, 609, 525
Coil A. L., Newman J. A., Cooper M. C., Davis M., Faber S. M., Koo D. C., Willmer C. N. A., 2006, ApJ, 644, 671
Coil A. L. et al., 2008, ApJ, 672, 153
Coles P., Jones B., 1991, MNRAS, 248, 1
Cooray A., Sheth R., 2002, Phys. Rep., 372, 1
Croton D. J. et al., 2006, MNRAS, 365, 11
de la Torre S. et al., 2007, A&A, 475, 443
de la Torre S. et al., 2009, preprint (arXiv:0911.2252)
De Lucia G., Blaizot J., 2007, MNRAS, 375, 2
De Lucia G., Kauffmann G., White S. D. M., 2004, MNRAS, 349, 1101
Fisher K. B., Davis M., Strauss M. A., Yahil A., Huchra J. P., 1994, MNRAS, 267, 927
Guzzo L. et al., 2007, ApJS, 172, 254
Iovino A. et al., 2010, A&A, 509, A40
Kaiser N., 1987, MNRAS, 227, 1
Kauffmann G., Haehnelt M., 2000, MNRAS, 311, 576
Kitzbichler M. G., White S. D. M., 2007, MNRAS, 376, 2
Koekemoer A. M. et al., 2007, ApJS, 172, 196
Kovač K. et al., 2009, preprint (arXiv:0910.0004)
Kovač K. et al., 2010, ApJ, 708, 505
Landy S. D., Szalay A. S., 1993, ApJ, 412, 64
Le Fèvre O. et al., 2003, in Iye M., Moorwood A. F. M., eds, Proc. SPIE Vol. 4841, Instrument Design and Performance for Optical/Infrared Ground-based Telescopes. SPIE, Bellingham, p. 1670
Le Fèvre O. et al., 2005, A&A, 439, 877
Lilly S. J. et al., 2007, ApJS, 172, 70
Lilly S. J. et al., 2009, ApJS, 184, 218
McCracken H. J. et al., 2007, ApJS, 172, 314
Marinoni C. et al., 2005, A&A, 442, 801
Meneux B. et al., 2006, A&A, 452, 387
Meneux B. et al., 2008, A&A, 478, 299
Meneux B. et al., 2009, A&A, 505, 463
Mo H. J., Jing Y. P., White S. D. M., 1996, MNRAS, 282, 1096
Narayanan V. K., Berlind A. A., Weinberg D. H., 2000, ApJ, 528, 1
Norberg P., Baugh C. M., Gaztañaga E., Croton D. J., 2009, MNRAS, 396, 19
Peebles P. J. E., 1980, The Large-scale Structure of the Universe. Princeton Univ. Press, Princeton, NJ
Pollo A. et al., 2006, A&A, 451, 409
Porciani C., Giavalisco M., 2002, ApJ, 565, 24
Scoville N. et al., 2007, ApJS, 172, 1
Sheth R. K., Tormen G., 1999, MNRAS, 308, 119
Sigad Y., Branchini E., Dekel A., 2000, ApJ, 540, 62
Smith R. E. et al., 2003, MNRAS, 341, 1311
Springel V., White S. D. M., Tormen G., Kauffmann G., 2001, MNRAS, 328, 726
Springel V. et al., 2005, Nat, 435, 629
Wang L., Steinhardt P. J., 1998, ApJ, 508, 483
White S. D. M., Frenk C. S., 1991, ApJ, 379, 52
York D. G. et al., 2000, AJ, 120, 1579

This paper has been typeset from a TEX/LATEX file prepared by the author.